Validation of IMERG precipitation in Africa

Amin K. Dezfuli[1,2], Charles M. Ichoku[1], George J. Huffman[1], Karen I. Mohr[1], John S. Selker[3], Nick van de Giesen[4], Rebecca Hochreutener[3], Frank O. Annor[4,5]

[1] NASA Goddard Space Flight Center

[2] Universities Space Research Association

[3] Biological and Ecological Engineering, Oregon State University

[4] Faculty of Civil Engineering and Geosciences, Delft University of Technology

[5] Civil Engineering Department, Kwame Nkrumah University of Science and Technology

Corresponding author: Amin K. Dezfuli (amin.dezfuli@nasa.gov)

Submitted to Journal of Hydrometeorology, September 2017

Abstract

Our understanding of hydroclimatic processes in Africa has been hindered by the lack of in-situ precipitation measurements. Satellite-based observations, in particular, the TRMM Multi-Satellite Precipitation Analysis (TMPA) have been pivotal to filling this void. The recently-released Integrated Multi-satellitE Retrievals for GPM (IMERG) project aims to continue the legacy of its predecessor, TMPA, and provide higher resolution data. Here, we validate IMERG-V04A precipitation data using in-situ observations from the Trans-African Hydro-Meteorological Observatory (TAHMO) project. Various evaluation measures are examined over a select number of stations in West and East Africa. In addition, continent-wide comparisons are made between IMERG and TMPA. The results show that the performance of the satellite-based products varies by season, region and the evaluation statistics. Precipitation diurnal cycle is relatively better captured by IMERG than TMPA. Both products exhibit a better agreement with gauge data in East Africa and humid West Africa than in the Southern Sahel. However, a clear advantage for IMERG is not apparent in detecting the annual cycle. Although all gridded products used here reasonably capture the annual cycle, some differences are evident during the short rains in East Africa. Direct comparison between IMERG and TMPA over the entire continent reveals that the similarity between the two products is also regionally heterogeneous. Except for Zimbabwe and Madagascar, where both satellite-based observations present a good agreement, the two products generally have their largest differences over mountainous regions. IMERG seems to have achieved a reduction in the positive bias evident in TMPA over Lake Victoria.

1. Introduction

Our knowledge about rainfall characteristics in Africa has been hampered by the lack of in-situ observations. (Figures 1a, S1). This is caused by a number of factors including restricted data-sharing policies and poor infrastructure due to economic vulnerability and long-lasting regional conflicts. Satellite-based precipitation observations have served as an alternative to fill this void, though insufficient ground-based rainfall records for calibration have posed some concerns for using these data sets. The TRMM Multi-Satellite Precipitation Analysis (TMPA), in particular has been successfully used in numerous studies (e.g., Beighley et al. 2011; Naumann et al. 2012; Dezfuli and Nicholson 2013; Munzimi et al. 2015; Ichoku et al. 2016). Built upon that success, the Global Precipitation Measurement (GPM) mission has been recently released by NASA and JAXA as a global successor to the TRMM project (Huffman et al. 2015). The Integrated Multi-satellitE Retrievals for GPM (IMERG), which incorporates observations from several satellites offers improvements over the TMPA in quality and spatio-temporal resolution of precipitation data (e.g., Ma et al. 2016; Prakash et al. 2016; Sharifi et al. 2016; Tang et al. 2016a). This is critical for enhancing our knowledge about various climatic phenomena in Africa that in addition to their regional implications have significant contribution to the global climate system (e.g., Swap et al. 1992; Kiladis et al. 2006; Dezfuli and Nicholson 2011; Lawrence and Vandecar 2015; Rivero-Calle et al. 2016). Performance of various aspects of the IMERG precipitation has been examined in different regions of the world (e.g., Liu 2016; Oliveira et al. 2016; Tan et al. 2016; Tang et al. 2016b; Asong et al. 2017). Such literature, however, is limited for Africa, primarily due to the lack of in-situ records (Hill et al. 2016; Sahlu et al. 2016; Dezfuli et al. 2017).

In this paper, we validate the half-hourly IMERG-V04A precipitation, using several weather stations in tropical Africa with very high temporal resolution. The diurnal variability, annual cycle, and frequency distribution of rain events from IMERG are compared with in-situ and several gridded precipitation products. These include TMPA, for which the intercomparison is performed on the spatial patterns of various evaluation measures over the entire continent of Africa. This study serves as a follow-up to our recent work (Dezfuli et al. 2017), in which the same in-situ data along with the IMERG and TMPA observations have been used to examine the characteristics of rain-producing systems in tropical Africa.

2. Precipitation Data

Various precipitation data sets are analyzed in order to have a comprehensive representation of major types of available products that are cited in the literature. These include five different data sets, obtained from a set of individual stations and four gridded products. Of these four, two are satellite-based (TMPA and IMERG), one is gauge-based (GPCC), and one is a blended gauge-satellite product (Climate Hazards Group InfraRed Precipitation with Station, CHIRPS).

The in-situ data is provided by the Trans-African Hydro-Meteorological Observatory (TAHMO). This recent initiative currently consists of about 100 low-cost weather stations, mainly in West and East Africa, and plans to grow its network to 20,000 stations across the entire continent (Van de Giesen et al. 2014). The TAHMO stations measure the standard meteorological variables at 5-minute intervals. Most stations, however, have data over a short period or are currently under quality control. We have selected three stations that met the quality control criteria and have data over the entire or most of the rainy season of 2015 (Figure 1b): Lela Primary School (LPS) in Kenya, Kumasi and Navrongo in Southern and Northern Ghana, respectively. Three additional

stations with a limited data period are also used only for analysis of diurnal variability. The stations are located within equatorial Africa, where meridional excursion of the tropical rainbelt creates a strong annual cycle of rainfall (Figure 1c-f; Dezfuli 2017).

The TMPA and IMERG data have been accessed from the NASA Precipitation Measurement Missions web portal at https://pmm.nasa.gov/. The TMPA-3B42(V7) product used here is available at daily and three hourly intervals and 0.25° spatial resolution. The IMERG product, which serves as the successor of TMPA, has a half-hourly temporal and 0.1° spatial resolution. The "Final Run" product of IMERG-V04A, which is calibrated with the GPCC gauge analysis, has been utilized. The GPCC First Guess Daily Product, available at 1° grid resolution (Schamm et al., 2014) is also used for data comparisons. This product incorporates precipitation records from weather stations across the globe (Figures 1a, S1), collected via the Global Telecommunication System (GTS). The CHIRPS data is used as the representative of the merged gauge-satellite products due to its high resolution, low bias, and good gauge-coverage over Africa, compared to other similar products (Funk et al., 2015). However, this expedited study does not intend to perform a full intercomparison among various data sets of this type, but to validate IMERG-V04A data using in-situ gauge measurements in parts of Africa where this has not been feasible hitherto, and to evaluate the performance of the current IMERG version vis-à-vis those of other comparable precipitation data sets. Several other gridded precipitation products that may be used for a more comprehensive inter-comparison analysis include Tropical Applications of Meteorology using SATellite (TAMSAT, Maidment et al. 2014), African Rainfall Climatology (ARC, Novella and Thiaw 2013), PERSIANN-CDR (Ashouri et al. 2015), GPCP (Adler et al. 2003) and CMORPH (Joyce et al. 2004).

3. Analysis Approach

Gridded data are spatially interpolated to the location of each TAHMO station for comparison. For each application, the mean precipitation rate over its associated interval is used. Annual cycles and probability distribution functions (PDF) of daily rainfall from various products are compared. The diurnal cycle is examined for three products with sub-daily records: TAHMO, IMERG, and TMPA. The TAHMO and IMERG data are averaged over the time range ±90 minutes from the nominal 3-hourly observation times used in TMPA. In addition, since IMERG is intended to replace TMPA, the spatial patterns of various evaluation measures of the two products are compared over the entire continent of Africa. These statistics include the correlation coefficient (CC), mean normalized absolute difference (MAD), multiplicative bias (mBias), probability of detection (POD), false alarm ratio (FAR), frequency bias (FBS), Critical Success Index (CSI), and Heidke skill score (HSS). For continent-wide spatial analysis, days with rainfall less than 1 mm are excluded in calculations of CC, MAD and mBias. The same threshold is used for categorical indices. For point analysis, a 0.2 mm threshold is applied, in order to ensure a sufficient number of dates required for the evaluation process. The definition of validation statistics, described in many references (e.g., Wilks, 2011), is provided in the Supplementary Materials using contingency Table S1. Considering reference data (e.g., in-situ observations), R, and the data that is validated, V, the POD is the ratio of the correct detection of rain events; FAR is the fraction of the days in V that are wrongly detected as rainy; FBS is the ratio of the number of rainy days in R to the number of rainy days in V; CSI is an accuracy measure that is particularly useful when the rainy days are substantially less frequent than the no-rain days; HSS is an accuracy measure that represents the proportion of correct matches between R and V to no-skill random matches.

4. Intercomparison of gauge and gridded data

Figures 2-4 show the evaluation results for LPS, Kumasi and Navrongo, respectively. Various validation measures, calculated for these stations, are provided in Tables 1, S2, and S3. The LPS, located in East Africa (Figure 2) has a bimodal annual cycle of rainfall. The two rainy seasons, occurring during March-April-May and October-November-December are known as "short rains" and "long rains", respectively. TMPA captures the annual cycle relatively better than IMERG, particularly during the short rains when differences are most noticeable among all the products. IMERG provides a better diurnal cycle than TMPA with respect to magnitude and temporal variation. The performance of both products varies by the season with improvements during the long rains (Figure 2c,d,e). However, the distribution of daily rainfall intensity provided by IMERG is very similar to that of the gauge observations, as evident in their PDFs and various percentiles (Figure 2f). The CHIRPS precipitation overall seems to have the largest differences with the gauge data, reflected in the short rains and the extreme daily rainfall rates.

The second TAHMO station, Kumasi (Figure 3), has also a bimodal annual cycle determined by the meridional excursion of the tropical rainbelt (e.g., Dezfuli 2017). Note that this station does not have data available during March and April. Although all products capture the month-to-month variability, some differences are noticeable in the rainfall magnitudes. For example, all gridded data underestimate the rainfall in May; CHIRPS is negatively biased in June; and IMERG presents an overestimation in December. The relatively better performance of TMPA than IMERG in representing the annual cycle is also reflected in the PDFs, where 90^{th} and 95^{th} percentiles of TMPA better agree with the in-situ observations (Figure 3f). The diurnal cycle of

148 rainfall, however, is reasonably well captured by both products throughout the year, though
149 IMERG offers some advantages over TMPA during February.
150 The third TAHMO station used here is Navrongo in Northern Ghana (Figure 4). This station,
151 located in the West African savanna, has a unimodal annual cycle with the peak rainy season
152 occurring during July-August-September (JAS). Although the annual cycle of various gridded
153 data sets has a good agreement with the in-situ observations, IMERG shows a relatively better
154 performance than the others. However, August that receives the maximum amount of rainfall is
155 overestimated by all products. The distribution of daily rainfall during April-October (Figure 4f)
156 is relatively better represented by the TMPA than other data sets, though IMERG's mean
157 intensity is equally close to the gauge data. The GPCC and CHIRPS have very similar PDFs. The
158 diurnal cycle is analyzed over three seasons (May-June, July-September, and October),
159 representing onset, peak and cessation of the West African Monsoon (WAM), respectively.
160 Although the temporal variation of diurnal cycle is fairly captured, the agreement between in-situ
161 and satellite-based observations is less than that shown for the other two stations, and several
162 differences are noticeable. However, important features such as the morning peak (06:00 LST)
163 during the JAS rainy season are detected. These rainfall characteristics are consistent with those
164 previously identified over the same region (Fink et al. 2006; Pfeifroth et al. 2016).
165 Three additional stations are also examined, two of which (Masindi, Uganda and Kapsabet,
166 Kenya) are located in East Africa and one (Enchi, Ghana) in West Africa (Fig. S2). Only diurnal
167 variability of rainfall was investigated using data from these stations, because availability of
168 continuous good quality records from them was limited to a two-month period. Enchi shows very
169 good agreement with both the IMERG and TMPA satellite products during the October-
170 November period. The diurnal cycle of the East African stations during the short-rains is also

171 reasonably similar to IMERG and TMPA, though some differences are apparent in the temporal
172 variation and magnitude of the rainfall rates. These differences are manifested as overestimation
173 by the satellite-based observations, mainly by IMERG at 03:00-06:00 LST in Masindi and by
174 TMPA at 18:00 LST in both stations.
175
176 **5. Spatial variability: IMERG vs. TMPA**
177 Various evaluation measures are examined for comparing IMERG and TMPA over the entire
178 continent of Africa (Figure 5). Each product is also separately compared with the GPCC daily
179 data (Figures S3, S4). This allows us to relate the IMERG-TMPA comparison patterns to
180 availability of the GPCC records, used for calibration of these products. Both IMERG and
181 TMPA show generally similar CC patterns with the GPCC. However, except for FAR, TMPA
182 seems to agree with GPCC slightly better than does IMERG. Of all the regions where GPCC
183 records exist, Zimbabwe and Madagascar present the highest agreement with both satellite-based
184 observations, consistent with previous studies (Dinku et al. 2008). Direct comparison between
185 IMERG and TMPA (Figure 5) reveals that the compatibility between the two products is also
186 regionally heterogeneous and varies by the evaluation measure. Note that IMERG has been
187 treated as the reference data in this comparison. Generally, the two products have their largest
188 differences in most parts of the Horn of Africa and over the Atlas Mountains and the adjacent
189 Mediterranean coastal area. These areas have the most complex terrain on the continent so the
190 distribution of gauges, product resolution, and the choice of retrieval algorithms would have a
191 significant impact. These differences are manifested primarily in the spatial patterns of MAD,
192 POD, FBS, CSI, and HSS. These statistics collectively represent the similarity between IMERG
193 and TMPA regarding the mean rainfall rate, detection of rain occurrences, and the accuracy of

194 correct matches relative to that of a no-skill random chance. The regions with the largest
195 differences in temporal variability of the two products, shown in CC patterns, generally appear
196 over the mountainous areas, although this is less evident in Angola and Tanzania. The spatial
197 patterns of CC, POD, FAR, FBS, and CSI show a strong consistency between IMERG and
198 TMPA over the Congo Basin and South Sudan. The four categorical statistics measure the
199 agreement in frequency of the daily rain occurrences. However, these regions are located in areas
200 with virtually no GPCC stations, implying that this agreement may not necessarily reflect the
201 quality of satellite observations. The mBias shows remarkably low values over Lake Victoria.
202 Similar results have been found for inland water bodies in China, where IMERG precipitation
203 values much more closely agree with the in-situ observations than does TMPA (Tang et al.
204 2016c). This improvement has been attributed to the unified and updated passive microwave
205 algorithm used in the GPM products.
206
207 **6. Discussion and Conclusions**
208 As a follow-up to our recent work (Dezfuli et al. 2017), we have used data from TAHMO to
209 improve our knowledge about rainfall characteristics in West and East Africa, validate the
210 IMERG-V04A precipitation data in these regions, and compare it with its successful predecessor
211 (TMPA) over the African continent. The complete areal coverage of satellite-based observations
212 is vital for capturing the intrinsic spatial heterogeneity of rainfall variability (Dezfuli 2011; Badr
213 et al. 2016) in the data-limited continent of Africa, and this can be further facilitated by the
214 potential of more in-situ measurements and ongoing improvements in IMERG. In addition,
215 IMERG can help us better understand the synoptic-scale meteorology of the region, as the
216 western and eastern parts of Africa have been shown to climatically communicate through

regional atmospheric circulation (Dezfuli et al. 2015). The high temporal resolution of in-situ and IMERG observations, in particular, has enabled us to better capture the regional variability of sub-daily rainfall. The results show that the diurnal cycle has a single-peak between 15:00-21:00 LST in East Africa and between 18:00-21:00 LST in Southern Ghana. However, the West African savanna exhibits a bimodal diurnal cycle that peaks at 06:00 and 18:00 LST during its rainy season, JAS, consistent with the previous studies over this region (Fink et al. 2006; Pfeifroth et al. 2016).

Although IMERG, partly due to its improved resolution, shows some advantages over TMPA in capturing the diurnal cycle, a clear superiority for other evaluation aspects cannot be claimed. In general, the choice of data set would depend on the region, season and objective of study. Various issues have made such decisions quite challenging. That includes the uncertainty due to the comparison of point and gridded data sets in this study, or the fact that we are not able to interpret the good agreement between IMERG and TMPA over the regions with no gauge records available for their calibration (the Congo Basin and South Sudan). In addition, this study is based on one year of data, which does not represent a full range of climate conditions. The growth of TAHMO network in coming years will hopefully help mitigate these issues and add to available gauge records, with potential usefulness for improving IMERG data that can offer significant contribution to understanding the climate processes in Africa and their implications to water, agriculture, and health sectors.

Acknowledgements

We thank the three anonymous reviewers for their constructive remarks. A.K.D.'s research was supported by the NASA Postdoctoral Program (NPP) at the Goddard Space Flight Center,

240 administrated by the Universities Space Research Association (USRA) through a contract with
241 NASA. This research was also supported under the NASA Research Opportunities in Space and
242 Earth Sciences (ROSES)–2009 and 2013 Interdisciplinary Studies (IDS) Program (Dr. Jack
243 Kaye, Earth Science Research Director), Grant NNH12ZDA001N-IDS, through the Radiation
244 Sciences Program managed by Dr.Hal Maring.
245
246 **References:**
247 Adler, R.F., Huffman, G.J., Chang, A., Ferraro, R., Xie, P.P., Janowiak, J., Rudolf, B.,
248 Schneider, U., Curtis, S., Bolvin, D. and Gruber, A., 2003. The version-2 global
249 precipitation climatology project (GPCP) monthly precipitation analysis (1979–
250 present). *Journal of hydrometeorology*, 4(6), pp.1147-1167.
251 Ashouri, H., Hsu, K.L., Sorooshian, S., Braithwaite, D.K., Knapp, K.R., Cecil, L.D., Nelson,
252 B.R. and Prat, O.P., 2015. PERSIANN-CDR: Daily precipitation climate data record
253 from multisatellite observations for hydrological and climate studies. *Bulletin of the*
254 *American Meteorological Society*, 96(1), pp.69-83.
255 Asong, Z.E., Razavi, S., Wheater, H.S. and Wong, J.S., 2017. Evaluation of Integrated
256 Multisatellite Retrievals for GPM (IMERG) over Southern Canada against Ground
257 Precipitation Observations: A Preliminary Assessment. *Journal of*
258 *Hydrometeorology*, *18*(4), pp.1033-1050.
259 Badr, H.S., Dezfuli, A.K., Zaitchik, B.F. and Peters-Lidard, C.D., 2016. Regionalizing Africa:
260 Patterns of Precipitation Variability in Observations and Global Climate Models. *Journal*
261 *of Climate*, *29*(24), pp.9027-9043.

Beighley, R.E., Ray, R.L., He, Y., Lee, H., Schaller, L., Andreadis, K.M., Durand, M., Alsdorf, D.E. and Shum, C.K., 2011. Comparing satellite derived precipitation datasets using the Hillslope River Routing (HRR) model in the Congo River Basin. *Hydrological Processes*, *25*(20), pp.3216-3229.

Dezfuli, A. K., 2017: Climate of western and central equatorial Africa. *Oxford Research Encyclopedia of Climate Science*, 66 pp., doi:10.1093/acrefore/9780190228620.013.511.

Dezfuli, A.K., 2011. Spatio-temporal variability of seasonal rainfall in western equatorial Africa. *Theoretical and applied climatology*, *104*(1-2), pp.57-69.

Dezfuli, A.K. and Nicholson, S.E., 2011. A note on long-term variations of the African easterly jet. *International Journal of Climatology*, *31*(13), pp.2049-2054.

Dezfuli, A.K. and Nicholson, S.E., 2013. The relationship of rainfall variability in western equatorial Africa to the tropical oceans and atmospheric circulation. Part II: The boreal autumn. *Journal of Climate*, *26*(1), pp.66-84.

Dezfuli, A.K., Zaitchik, B.F. and Gnanadesikan, A., 2015. Regional atmospheric circulation and rainfall variability in south equatorial Africa. *Journal of Climate*, *28*(2), pp.809-818.

Dezfuli, A.K., Ichoku, C.M., Mohr, K. and Huffman, G.J., 2017. Precipitation characteristics in West and East Africa, from satellite and in-situ observations. *Journal of Hydrometeorology*, (2017).

Dezfuli, A.K., 2017. Climate of Western and Central Equatorial Africa. *Oxford Research Encyclopedia of Climate Science*, doi: 10.1093/acrefore/9780190228620.013.511

Dinku, T., Chidzambwa, S., Ceccato, P., Connor, S.J. and Ropelewski, C.F., 2008. Validation of high-resolution satellite rainfall products over complex terrain. *International Journal of Remote Sensing*, *29*(14), pp.4097-4110.

285 Fink, A.H., Vincent, D.G. and Ermert, V., 2006. Rainfall types in the West African Sudanian
286 zone during the summer monsoon 2002. *Monthly weather review*, 134(8), pp.2143-2164.
287 Funk, C., Peterson, P., Landsfeld, M., Pedreros, D., Verdin, J., Shukla, S., Husak, G., Rowland,
288 J., Harrison, L., Hoell, A. and Michaelsen, J., 2015. The climate hazards infrared
289 precipitation with stations--a new environmental record for monitoring
290 extremes. *Scientific data*, *2*, p.150066.
291 Hill, P.G., Allan, R.P., Chiu, J.C. and Stein, T.H., 2016. A multisatellite climatology of clouds,
292 radiation, and precipitation in southern West Africa and comparison to climate
293 models. *Journal of Geophysical Research: Atmospheres*, *121*(18).
294 Huffman, G.J., Bolvin, D.T. and Nelkin, E.J., 2015. Day 1 IMERG final run release notes. *NASA*
295 *Goddard Earth Sciences Data and Information Services Center: Greenbelt, MD, USA*.
296 Ichoku, C., Ellison, L.T., Willmot, K.E., Matsui, T., Dezfuli, A.K., Gatebe, C.K., Wang, J.,
297 Wilcox, E.M., Lee, J., Adegoke, J. and Okonkwo, C., 2016. Biomass burning, land-cover
298 change, and the hydrological cycle in Northern sub-Saharan Africa. *Environmental*
299 *Research Letters*, *11*(9), p.095005.
300 Joyce, R.J., Janowiak, J.E., Arkin, P.A. and Xie, P., 2004. CMORPH: A method that produces
301 global precipitation estimates from passive microwave and infrared data at high spatial
302 and temporal resolution. *Journal of Hydrometeorology*, 5(3), pp.487-503.
303 Kiladis, G.N., Thorncroft, C.D. and Hall, N.M., 2006. Three-dimensional structure and dynamics
304 of African easterly waves. Part I: Observations. *Journal of the atmospheric*
305 *sciences*, *63*(9), pp.2212-2230.
306 Lawrence, D. and Vandecar, K., 2015. Effects of tropical deforestation on climate and
307 agriculture. *Nature Climate Change*, *5*(1), pp.27-36.

Liu, Z., 2016. Comparison of Integrated Multisatellite Retrievals for GPM (IMERG) and TRMM Multisatellite Precipitation Analysis (TMPA) Monthly Precipitation Products: Initial Results. *Journal of Hydrometeorology*, *17*(3), pp.777-790.

Ma, Y., Tang, G., Long, D., Yong, B., Zhong, L., Wan, W. and Hong, Y., 2016. Similarity and Error Intercomparison of the GPM and Its Predecessor-TRMM Multisatellite Precipitation Analysis Using the Best Available Hourly Gauge Network over the Tibetan Plateau. *Remote Sensing*, *8*(7), p.569.

Maidment, R.I., Grimes, D., Allan, R.P., Tarnavsky, E., Stringer, M., Hewison, T., Roebeling, R. and Black, E., 2014. The 30 year TAMSAT African rainfall climatology and time series (TARCAT) data set. *Journal of Geophysical Research: Atmospheres*, 119(18).

Munzimi, Y.A., Hansen, M.C., Adusei, B. and Senay, G.B., 2015. Characterizing congo basin rainfall and climate using tropical rainfall measuring mission (trmm) satellite data and limited rain gauge ground observations. *Journal of Applied Meteorology and Climatology*, *54*(3), pp.541-555.

Naumann, G., Barbosa, P., Carrao, H., Singleton, A. and Vogt, J., 2012. Monitoring drought conditions and their uncertainties in Africa using TRMM data. *Journal of Applied meteorology and Climatology*, *51*(10), pp.1867-1874.

Novella, N.S. and Thiaw, W.M., 2013. African rainfall climatology version 2 for famine early warning systems. *Journal of Applied Meteorology and Climatology*, 52(3), pp.588-606.

Oliveira, R., Maggioni, V., Vila, D. and Morales, C., 2016. Characteristics and Diurnal Cycle of GPM Rainfall Estimates over the Central Amazon Region. *Remote Sensing*, *8*(7), p.544.

329 Pfeifroth, U., Trentmann, J., Fink, A.H. and Ahrens, B., 2016. Evaluating satellite-based diurnal
330 cycles of precipitation in the African tropics. *Journal of Applied Meteorology and*
331 *Climatology*, 55(1), pp.23-39.
332 Prakash, S., Mitra, A.K., Pai, D.S. and AghaKouchak, A., 2016. From TRMM to GPM: How
333 well can heavy rainfall be detected from space?. *Advances in Water Resources*, *88*, pp.1-
334 7.
335 Rivero-Calle, S., Del Castillo, C.E., Gnanadesikan, A., Dezfuli, A., Zaitchik, B. and Johns, D.G.,
336 2016. Interdecadal Trichodesmium variability in cold North Atlantic waters. *Global*
337 *Biogeochemical Cycles*, *30*(11), pp.1620-1638.
338 Sahlu, D., Nikolopoulos, E.I., Moges, S.A., Anagnostou, E.N. and Hailu, D., 2016. First
339 Evaluation of the Integrated Multi-satellitE Retrieval for GPM Day-1 IMERG over the
340 upper Blue Nile Basin. *Journal of Hydrometeorology*, (2016).
341 Schamm, K., Ziese, M., Becker, A., Finger, P., Meyer-Christoffer, A., Schneider, U., Schröder,
342 M. and Stender, P., 2014. Global gridded precipitation over land: a description of the new
343 GPCC First Guess Daily product. *Earth System Science Data*, *6*(1), pp.49-60.
344 Sharifi, E., Steinacker, R. and Saghafian, B., 2016. Assessment of GPM-IMERG and Other
345 Precipitation Products against Gauge Data under Different Topographic and Climatic
346 Conditions in Iran: Preliminary Results. *Remote Sensing*, *8*(2), p.135.
347 Swap, R., Garstang, M., Greco, S., Talbot, R. and Kållberg, P., 1992. Saharan dust in the
348 Amazon Basin. *Tellus B*, *44*(2), pp.133-149.
349 Tan, J., Petersen, W.A. and Tokay, A., 2016. A Novel Approach to Identify Sources of Errors in
350 IMERG for GPM Ground Validation. *Journal of Hydrometeorology*, *17*(9), pp.2477-
351 2491.

352 Tang, G., Ma, Y., Long, D., Zhong, L. and Hong, Y., 2016a. Evaluation of GPM Day-1 IMERG
353 and TMPA Version-7 legacy products over Mainland China at multiple spatiotemporal
354 scales. *Journal of Hydrology*, *533*, pp.152-167.
355 Tang, G., Zeng, Z., Long, D., Guo, X., Yong, B., Zhang, W. and Hong, Y., 2016b. Statistical and
356 Hydrological Comparisons between TRMM and GPM Level-3 Products over a
357 Midlatitude Basin: Is Day-1 IMERG a Good Successor for TMPA 3B42V7?. *Journal of*
358 *Hydrometeorology*, *17*(1), pp.121-137.
359 Tang, G., Long, D. and Hong, Y., 2016c. Systematic anomalies over inland water bodies of High
360 Mountain Asia in TRMM precipitation estimates: No longer a problem for the GPM era?.
361 *IEEE Geoscience and Remote Sensing Letters*.
362 Van de Giesen, N., Hut, R. and Selker, J., 2014. The Trans-African Hydro-Meteorological
363 Observatory (TAHMO). *Wiley Interdisciplinary Reviews: Water*, *1*(4), pp.341-348.
364 Wilks, D.S., 2011. *Statistical methods in the atmospheric sciences* (Vol. 100). Academic press.

Table 1. Evaluation measures based on daily data for IMERG and TMPA at three TAHMO's stations for the months in 2015 with available in-situ observations. Days with rainfall less than 0.2 mm are excluded in calculations of CC, MAD and mBias. The same threshold is used in contingency table of the categorical statistics. This threshold ensures a sufficient number of dates, required for evaluation process.

Station	Period	Data	CC	MAD	mBias	POD	FAR	FBS	CSI	HSS
LPS, KE	Feb-Dec	IMERG	.54	.81	1.04	.84	.17	1.02	.71	.58
		TMPA	.55	.83	1.08	.81	.20	1.01	.68	.53
Kumasi, GH	Feb-Nov	IMERG	.42	.83	.73	.73	.35	1.12	.52	.38
		TMPA	.57	.82	.85	.72	.32	1.06	.54	.42
Navrongo, GH	Apr-Oct	IMERG	.62	.80	1.01	.64	.20	.80	.55	.53
		TMPA	.54	.86	.92	.69	.27	.95	.55	.50

Figures

Figure 1. (a) Mean number of stations per month used in GPCC First Guess Daily product during 2015. (b) Location of the TAHMO weather stations. For Stations Set 1, annual cycle, diurnal cycle and probability density function of daily rainfall are examined. For Stations Set 2, only diurnal cycle is examined. (c-f) Long-term mean (1998-2015) patterns of monthly precipitation, using TMPA 3B42 data.

Figure 2. (a) Location of the station of interest (yellow square), Lela Primary School (LPS) in Kenya, and other stations (purple circles). (b) Annual cycle of rainfall for various data sets during 2015. (c-e) Diurnal cycle of rainfall for LPS, IMERG and TMPA in three different seasons. Blue dashed lines (TMPA_LTM), shown in b-e represent long-term mean of annual and diurnal cycles, based on TMPA data over 1998-2015. These are used to determine the condition of year 2015 relative to the climatology. (f) Probability density function of daily rainfall for various data sets; white circle shows the mean and horizontal lines represent different percentiles. All gridded data are spatially interpolated to the location of the station.

Figure 3. The same as Figure 2, but for Kumasi, Ghana.

Figure 4. The same as Figure 2, but for Navrongo, Ghana.

Figure 5. (a) Topographic map of Africa. (b-i) Various validation measures used for comparison between IMERG and TMPA during 2015. IMERG is considered as reference data. Grids with a large number of zero daily rainfall values are masked, using some restricting criteria (see Supplementary Materials).

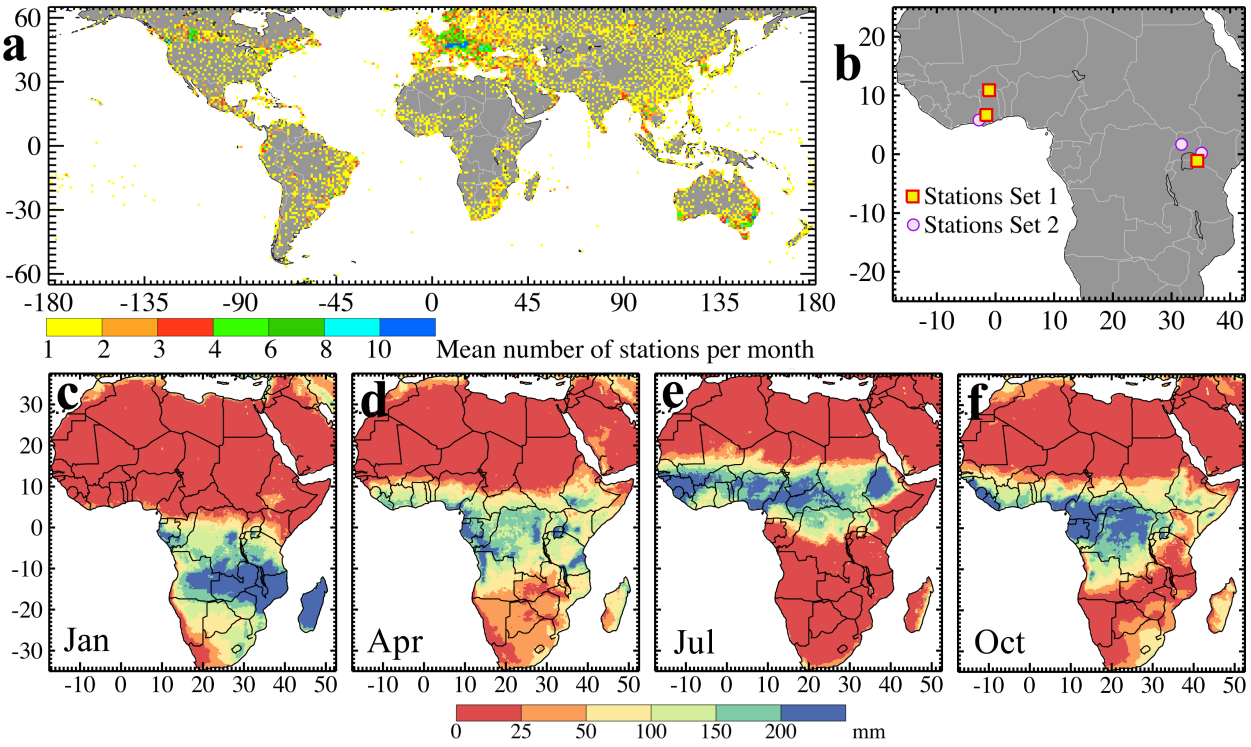

Figure 1. (a) Mean number of stations per month used in GPCC First Guess Daily product during 2015. (b) Location of the TAHMO weather stations. For Stations Set 1, annual cycle, diurnal cycle and probability density function of daily rainfall are examined. For Stations Set 2, only diurnal cycle is examined. (c-f) Long-term mean (1998-2015) patterns of monthly precipitation, using TMPA 3B42 data.

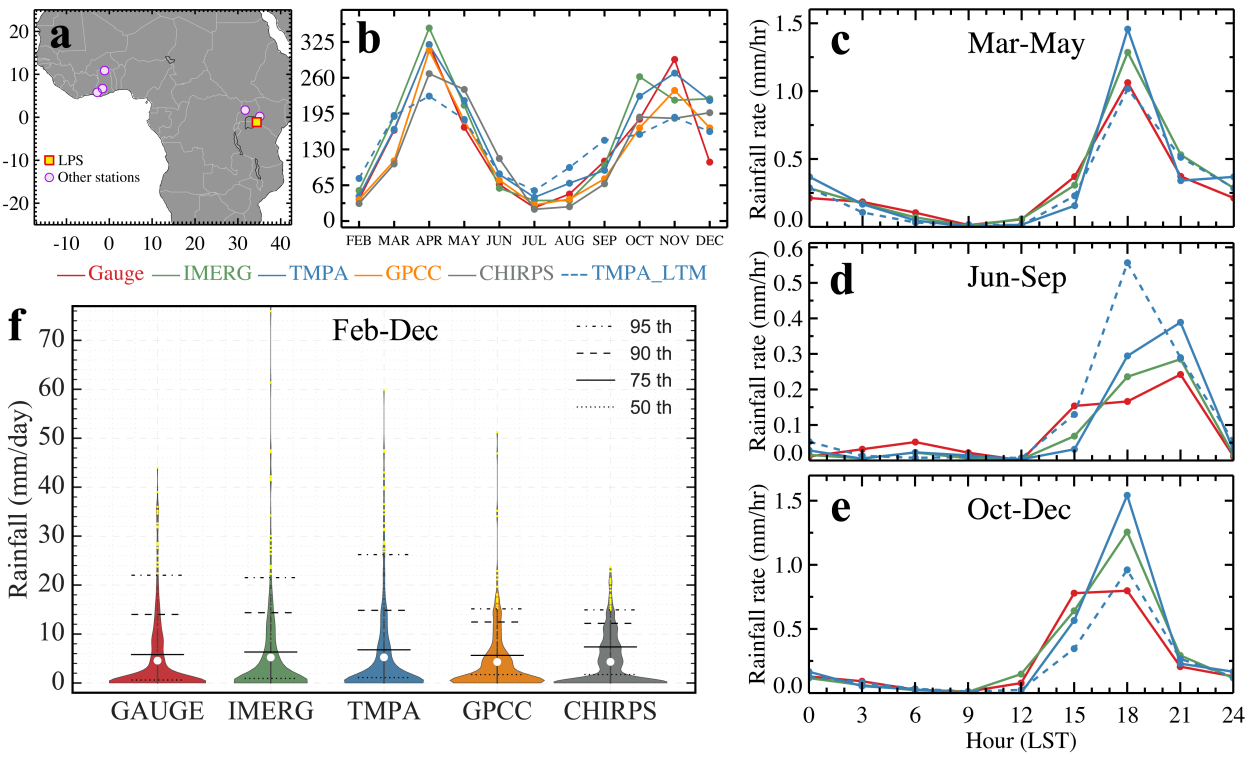

Figure 2. (a) Location of the station of interest (yellow square), Lela Primary School (LPS) in Kenya, and other stations (purple circles). (b) Annual cycle of rainfall for various data sets during 2015. (c-e) Diurnal cycle of rainfall for LPS, IMERG and TMPA in three different seasons. Blue dashed lines (TMPA_LTM), shown in b-e represent long-term mean of annual and diurnal cycles, based on TMPA data over 1998-2015. These are used to determine the condition of year 2015 relative to the climatology. (f) Probability density function of daily rainfall for various data sets; white circle shows the mean and horizontal lines represent different percentiles. All gridded data are spatially interpolated to the location of the station.

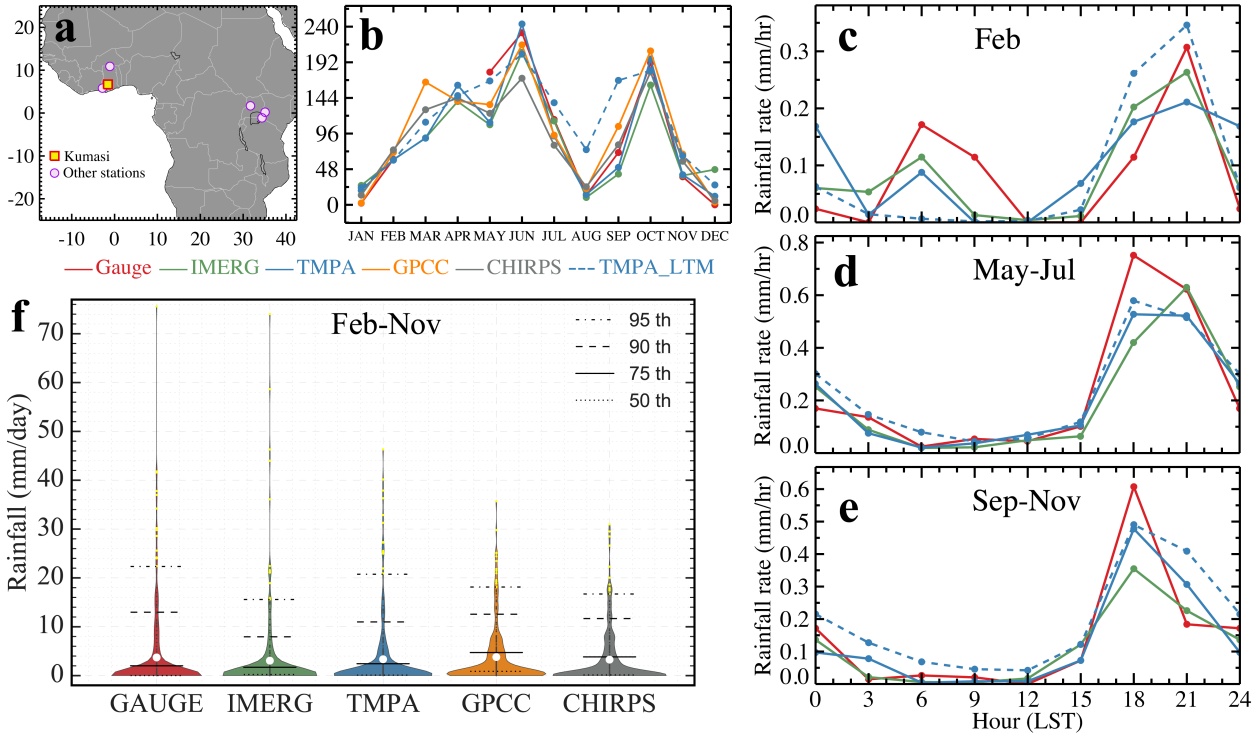

406

407 **Figure 3.** The same as Figure 2, but for Kumasi, Ghana.

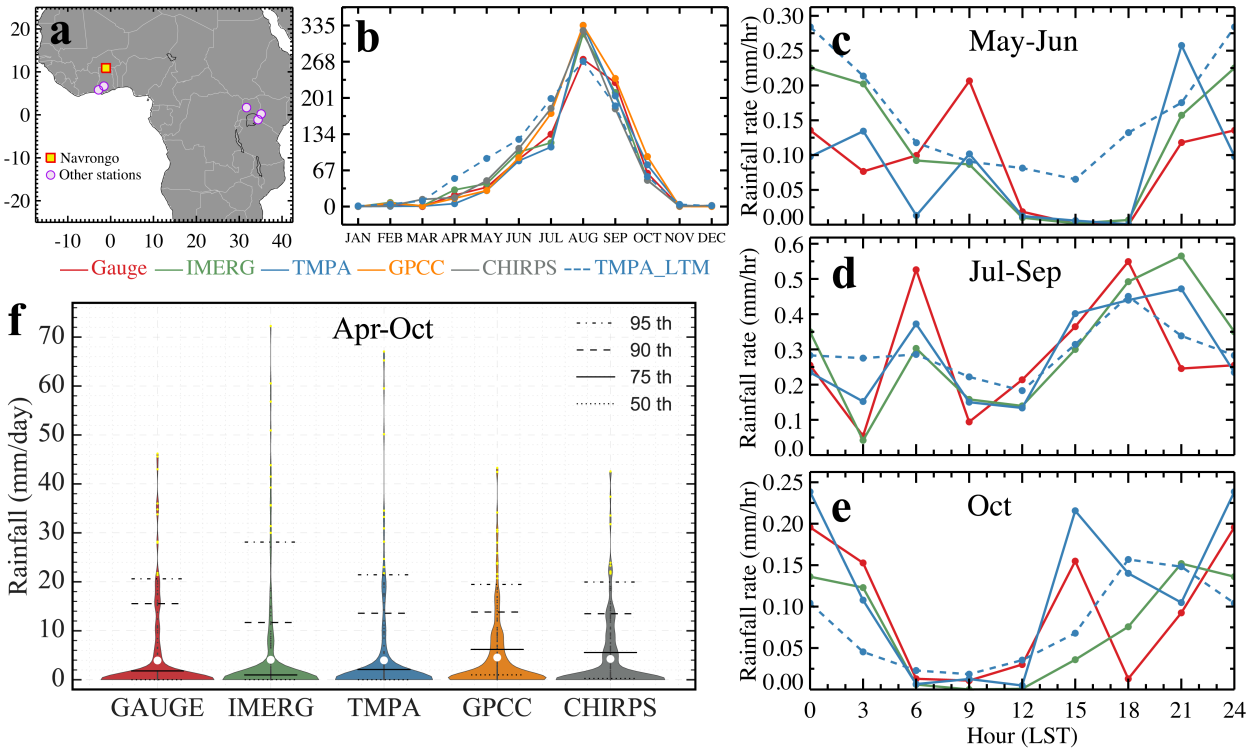

408

409 **Figure 4.** The same as Figure 2, but for Navrongo, Ghana.

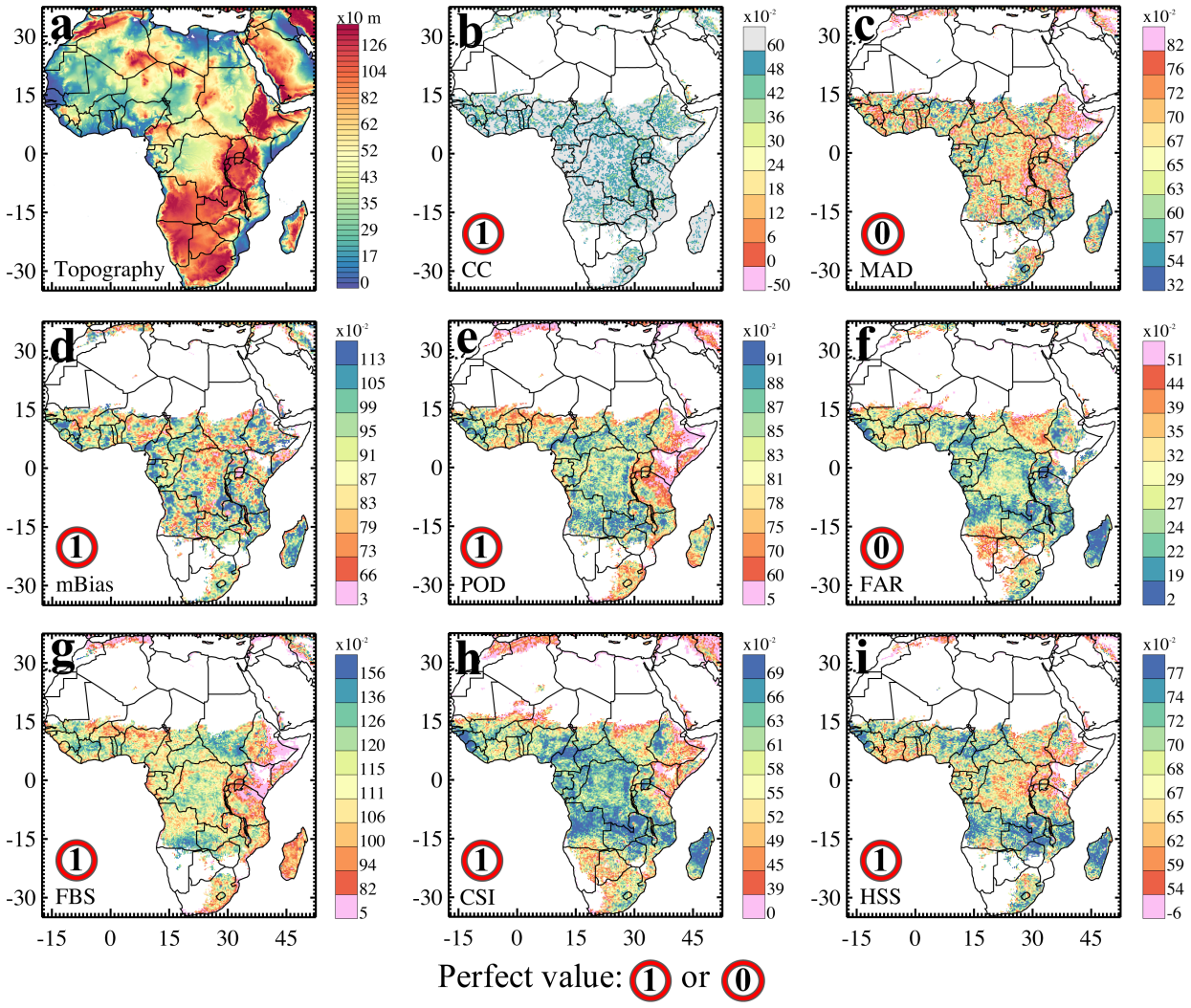

410

411 **Figure 5.** (a) Topographic map of Africa. (b-i) Various validation measures used for comparison

412 between IMERG and TMPA during 2015. IMERG is considered as reference data. Grids with a

413 large number of zero daily rainfall values are masked, using some restricting criteria (see

414 Supplementary Materials).